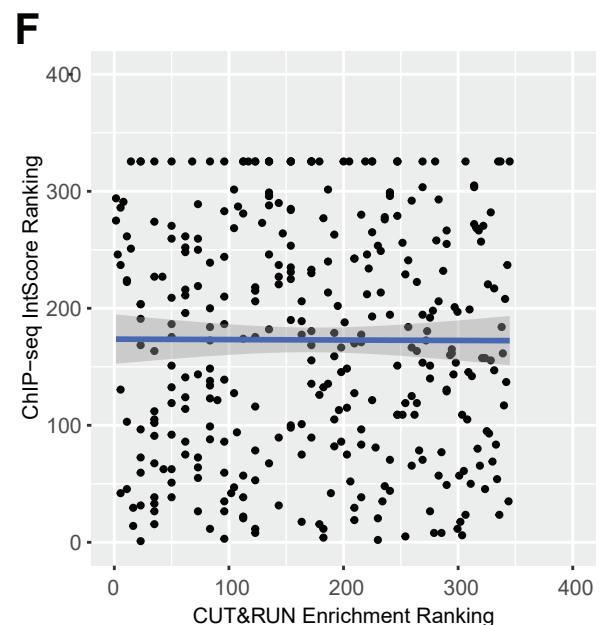
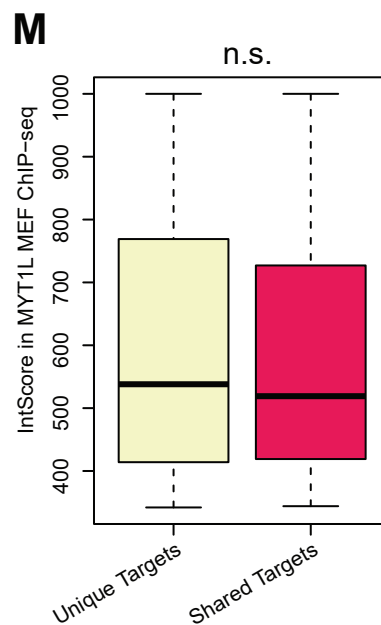
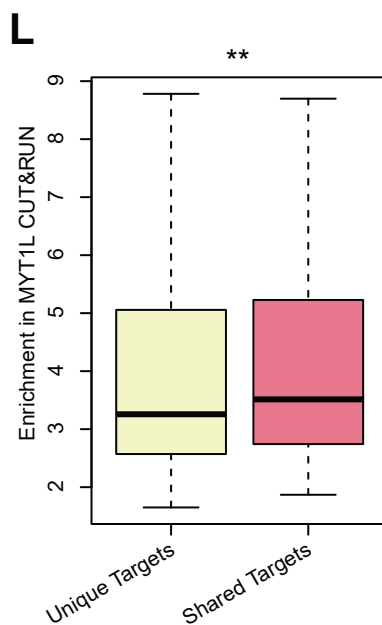
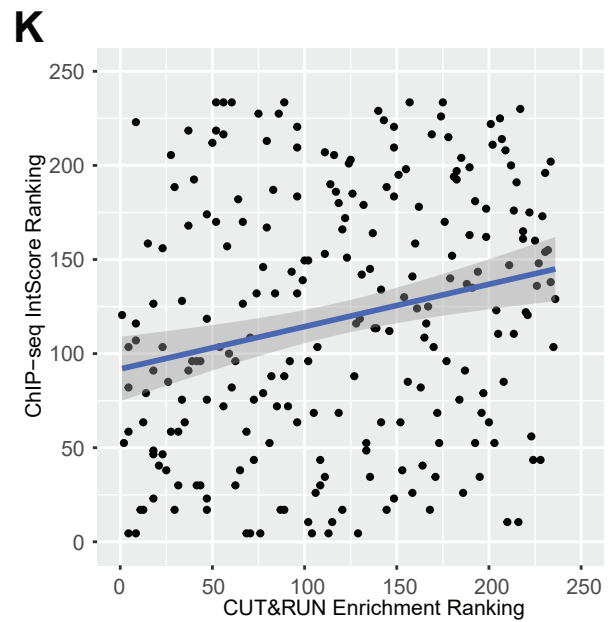
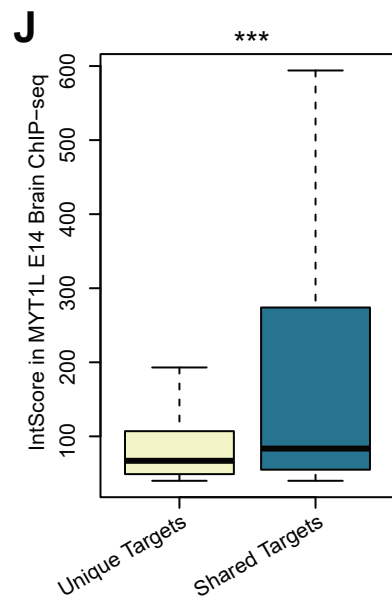
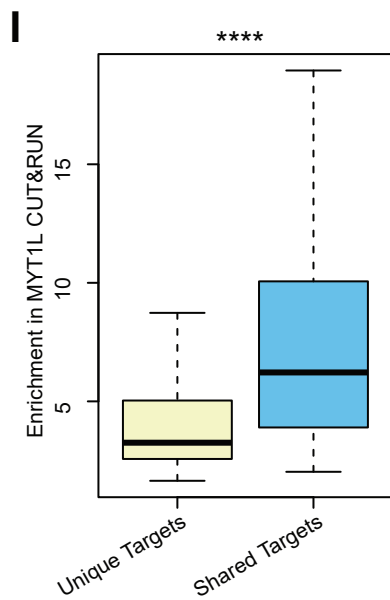
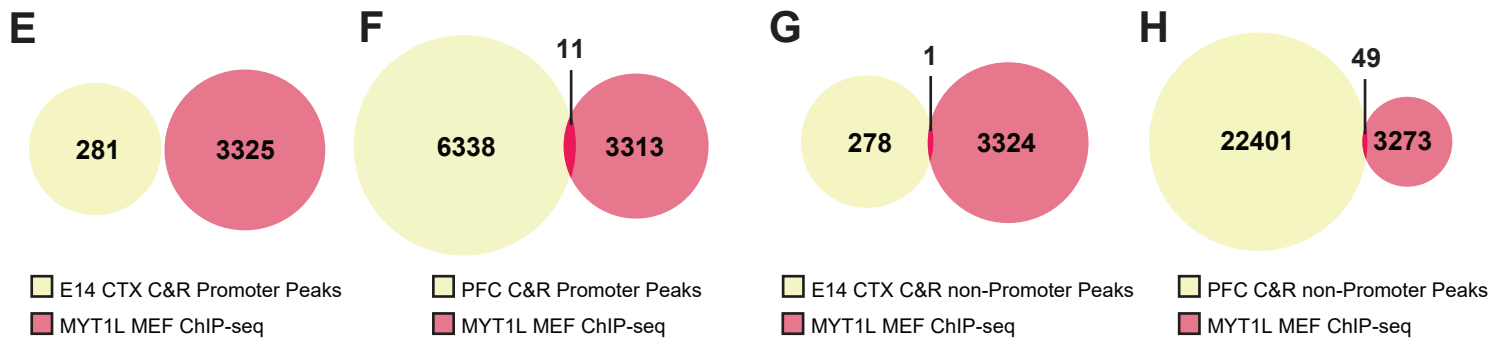
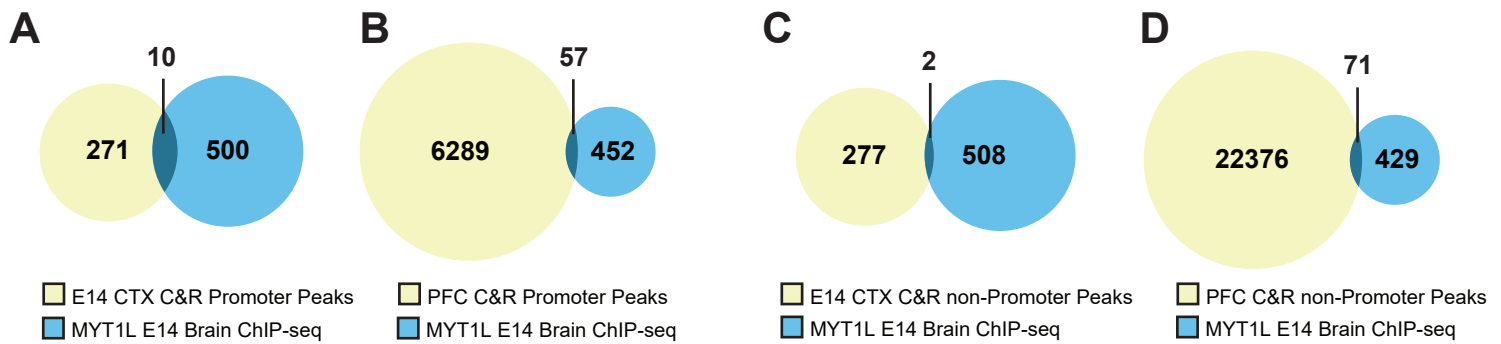
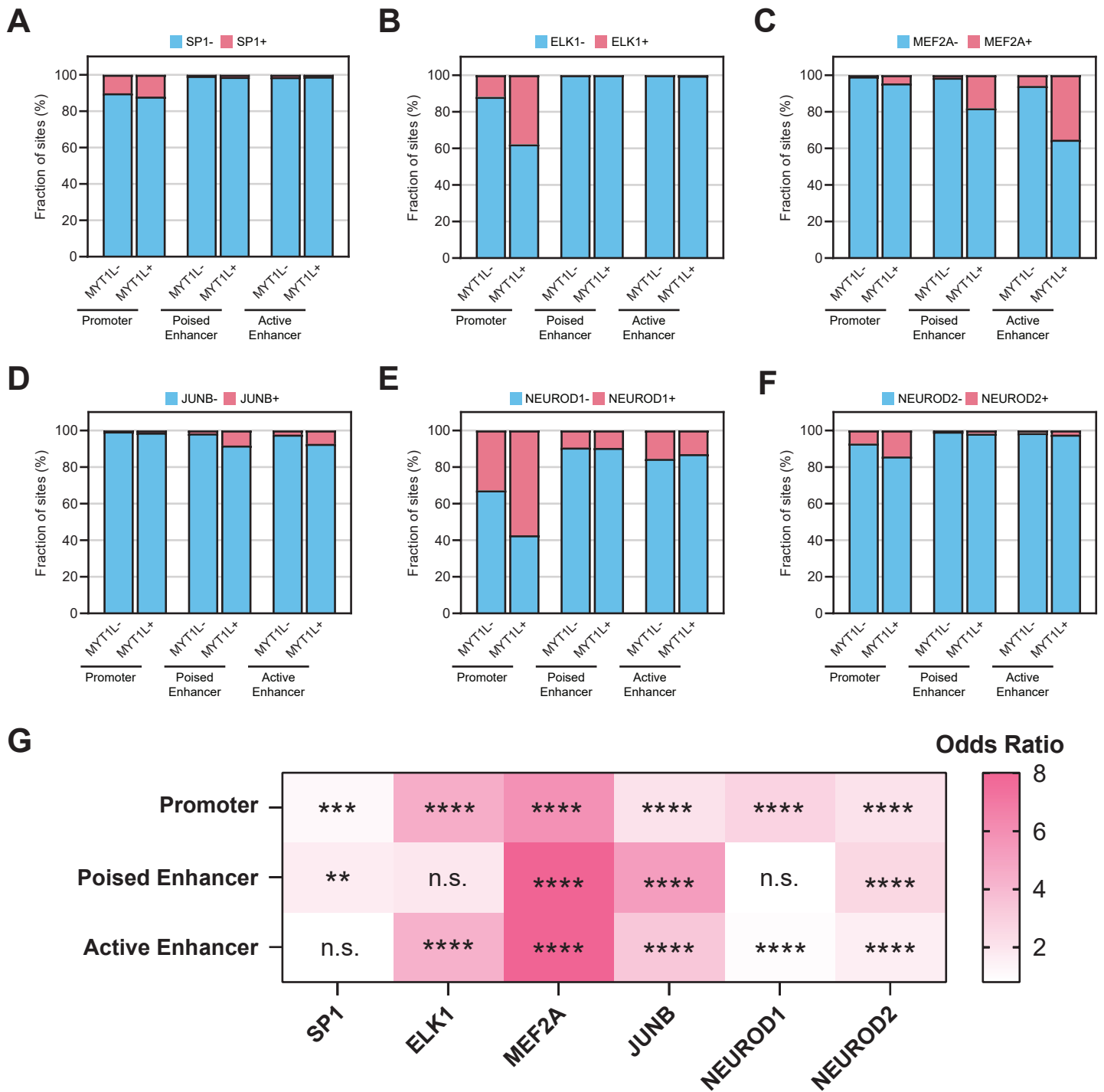


Supplemental Figure 1: CUT&RUN is more efficient for MYT1L binding profiling on P60 PFC than on E14 CTX.

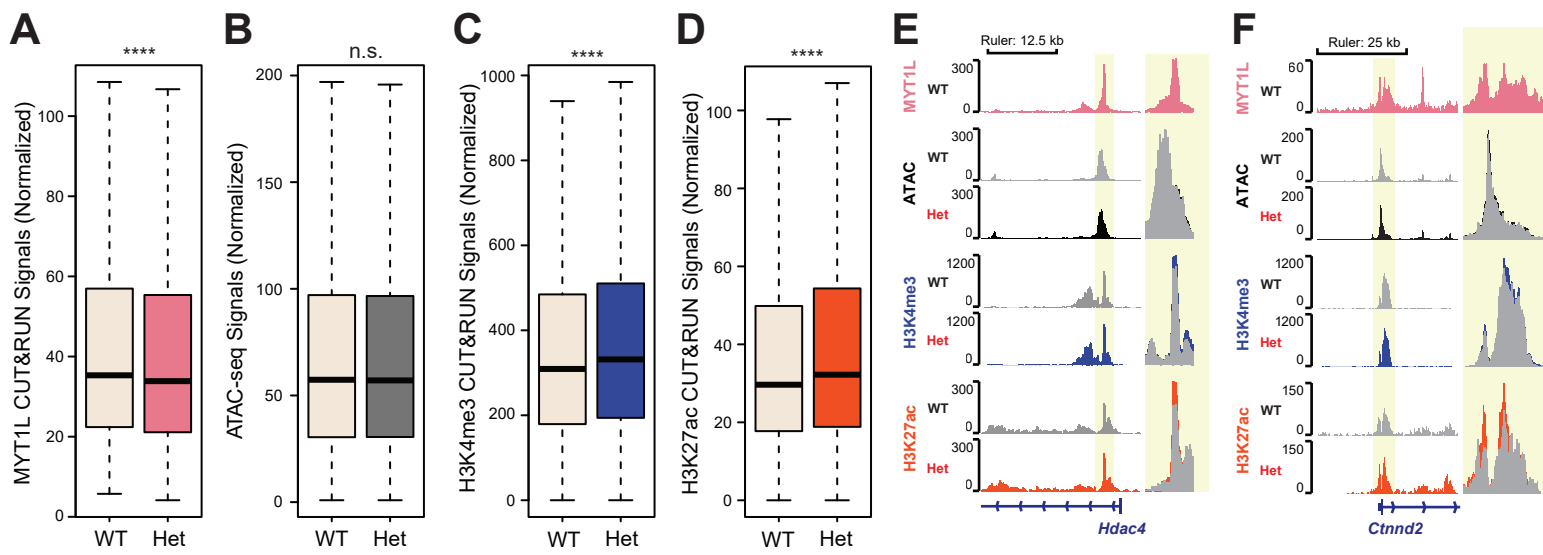
(A) Homer de novo motif finding shows significant enrichment of MYT1L core binding motif AAGTT in E14 MYT1L CUT&RUN peaks. (B) Homer de novo motif finding shows significant enrichment of MYT1L core binding motif AAGTT in PFC MYT1L CUT&RUN peaks. (C) Overlaps between MYT1L PFC and E14 CUT&RUN promoter peaks. (D) Overlaps between MYT1L PFC and E14 CUT&RUN non-promoter peaks.



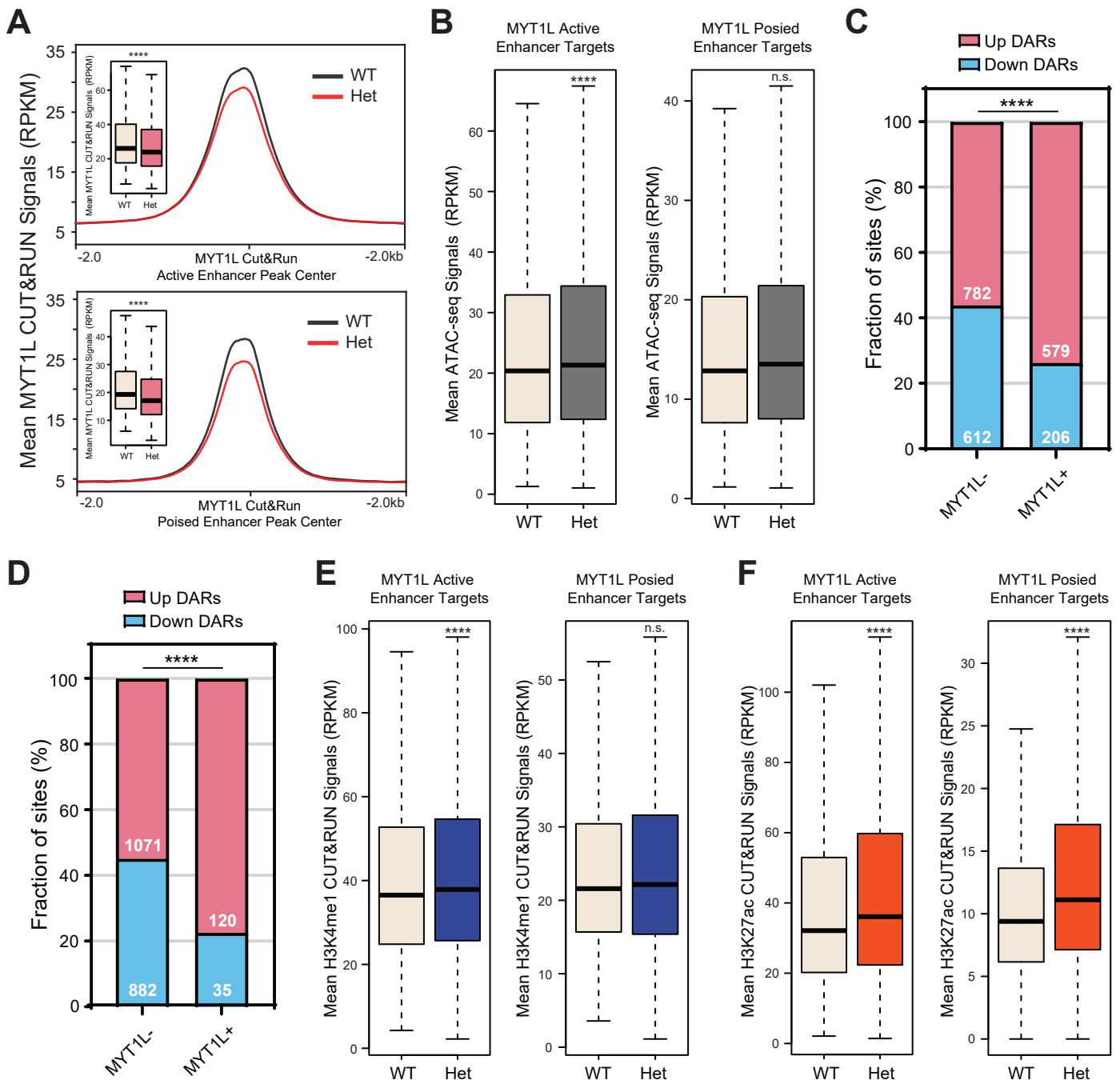
Supplemental Figure 2: MYT1L CUT&RUN on E14 CTX and adult PFC poorly overlaps with MYT1L ChIP-seq on E14 mouse brain and MEFs. (A) No significant overlap was found between MYT1L E14 CTX CUT&RUN promoter peaks and MYT1L E14 brain ChIP-seq peaks. (B) No significant overlap was found between MYT1L PFC CUT&RUN promoter peaks and MYT1L E14 brain ChIP-seq peaks. (C) No significant overlap was found between MYT1L E14 CTX CUT&RUN non-promoter peaks and MYT1L E14 brain ChIP-seq peaks. (D) No significant overlap was found between MYT1L PFC CUT&RUN non-promoter peaks and MYT1L E14 brain ChIP-seq peaks. (E) No significant overlap was found between MYT1L E14 CTX CUT&RUN promoter peaks and MYT1L MEF ChIP-seq peaks. (F) No significant overlap was found between MYT1L PFC CUT&RUN promoter peaks and MYT1L MEF ChIP-seq peaks. (G) No significant overlap was found between MYT1L E14 CTX CUT&RUN non-promoter peaks and MYT1L MEF ChIP-seq peaks. (H) No significant overlap was found between MYT1L PFC CUT&RUN non-promoter peaks and MYT1L MEF ChIP-seq peaks. (I) Boxplot of peak enrichment from MYT1L PFC CUT&RUN for shared targets between CUT&RUN and E14 brain ChIP-seq. (J) Boxplot of peak scores from MYT1L E14 brain ChIP-seq for shared targets between CUT&RUN and E14 brain ChIP-seq. (K) Spearman's rank correlation of shared targets in two datasets ($p = 0.00049$, $\rho = 0.22$). (L) Boxplot of peak enrichment from MYT1L PFC CUT&RUN for shared targets between CUT&RUN and MEF ChIP-seq. (M) Boxplot of peak scores from MYT1L E14 brain ChIP-seq for shared targets between CUT&RUN and MEF ChIP-seq. (N) Spearman's rank correlation of shared targets in two datasets ($p = 0.94$, $\rho = -0.0037$). * $p < 0.05$, ** $p < 0.01$, *** $p < 0.001$, **** $p < 0.0001$.



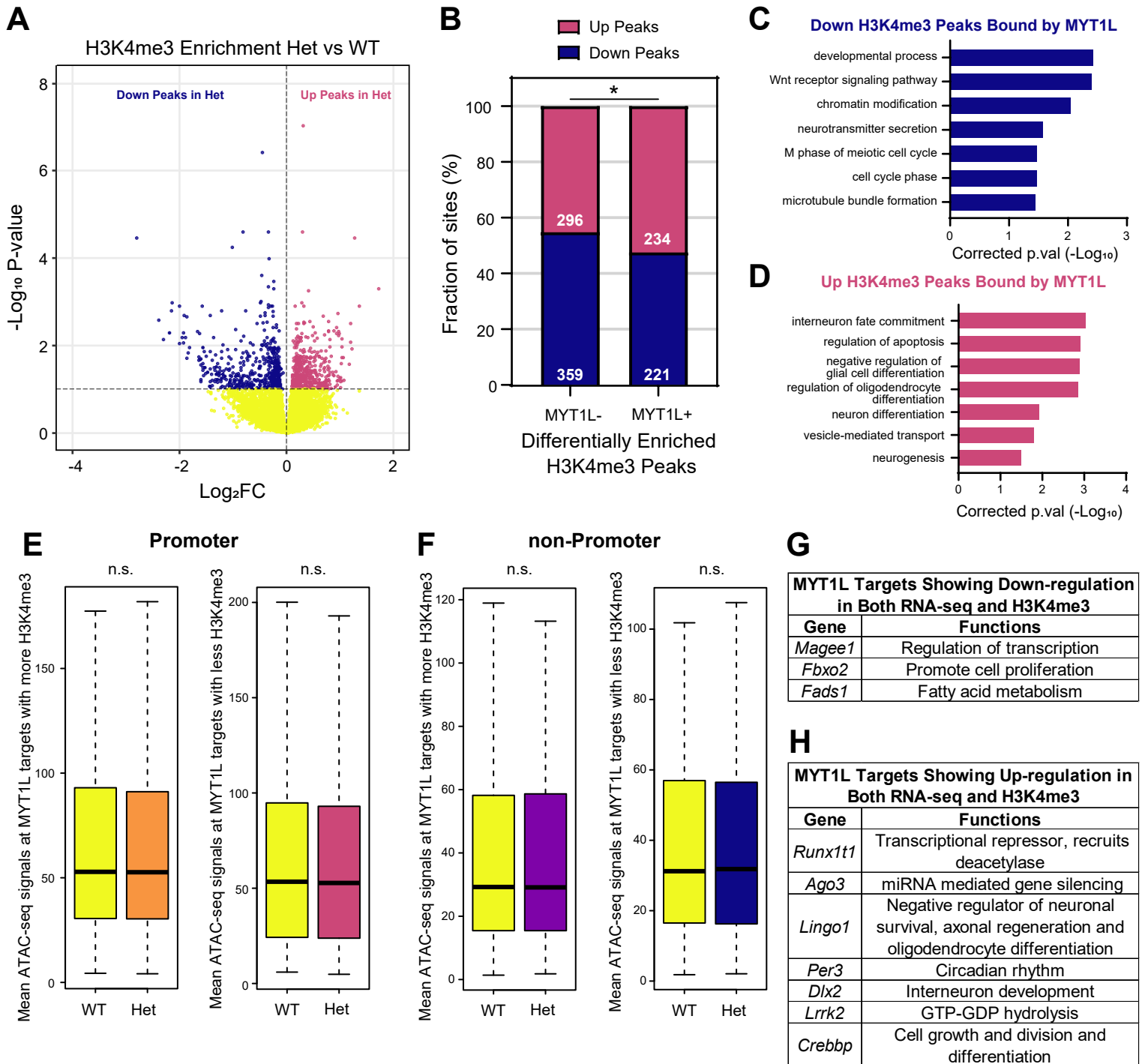
Supplemental Figure 3: MYT1L co-occupies with a different set of transcriptional factors at promoters and enhancers. (A) MYT1L+ promoters have a significantly higher percentage of SP1 binding compared to MYT1L- promoters, while no obvious difference was observed in enhancers. The same pattern was observed for (B) ELK1 as well. (C) MYT1L+ enhancers have a significantly higher percentage of MEF2A binding compared to MYT1L- promoters, while no big difference was observed in promoters. The same pattern was observed for (D) JUNB as well. (E) MYT1L+ promoters have a significantly higher percentage of NEUROD1 binding compared to MYT1L- promoters, while no obvious difference was observed in enhancers. The same pattern was observed for (F) NEUROD2 as well. (G) Fisher's exact test showed different TFs' enrichment in MYT1L+ over MYT1L- genomic regions. * $p < 0.05$, ** $p < 0.01$, *** $p < 0.001$, **** $p < 0.0001$.



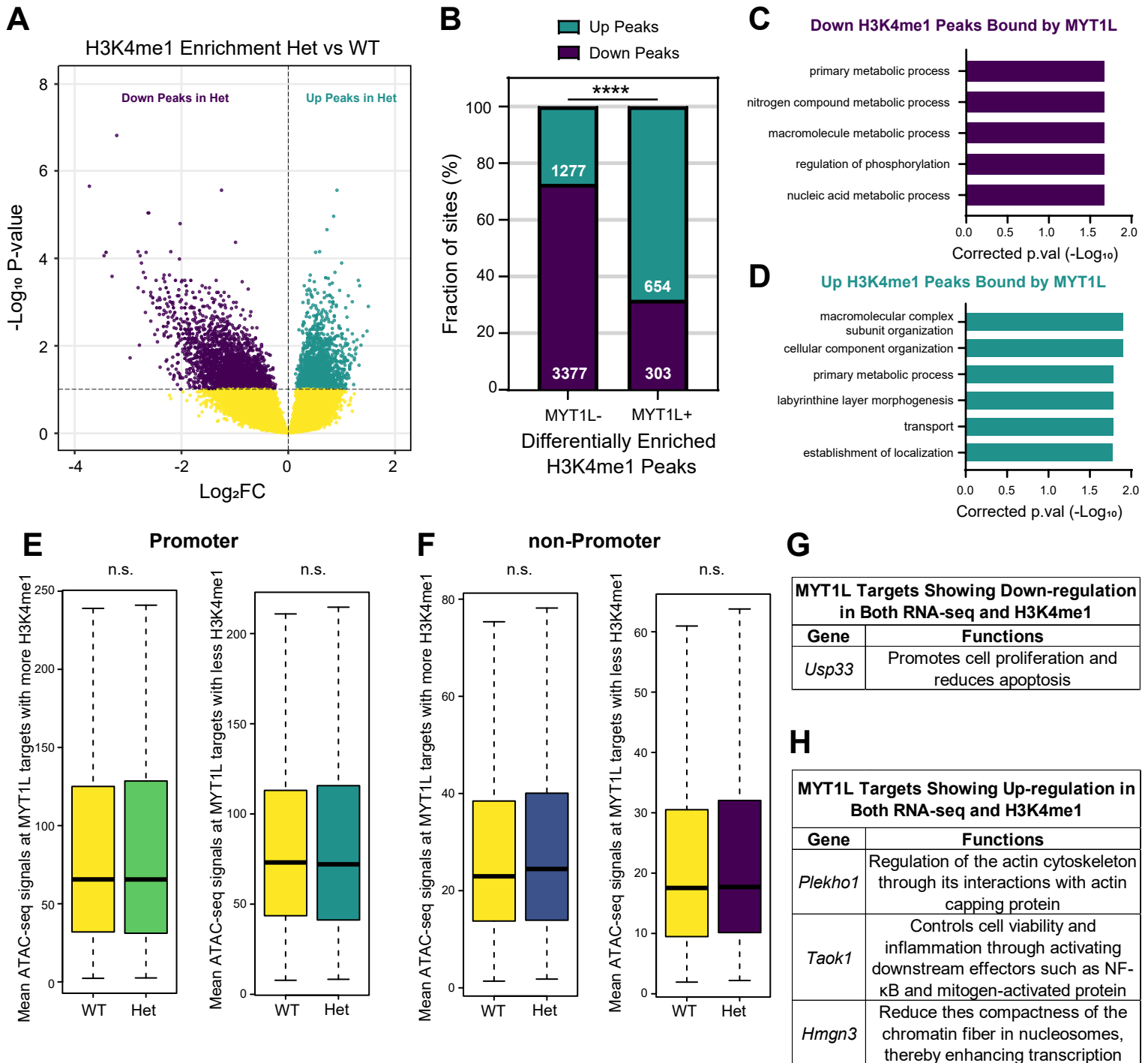
Supplemental Figure 4: MYT1L loss increases H3K4me3 and H3K27ac levels at promoters. (A) Het PFC showed decreased MYT1L CUT&RUN signals at MYT1L bound promoters. (B) MYT1L loss did not alter its bound promoters' chromatin accessibility. (C) MYT1L Het PFC has higher levels of H3K4me3 at MYT1L promoter targets compared to WTs. (D) MYT1L Het PFC has higher levels of H3K27ac at MYT1L promoter targets compared to WTs. (E) Representative genome browser track of MYT1L bound *Hdac4* promoter. (F) Representative genome browser track of MYT1L bound *Ctnnd2* promoter.
* $p < 0.05$, ** $p < 0.01$, *** $p < 0.001$, **** $p < 0.0001$.



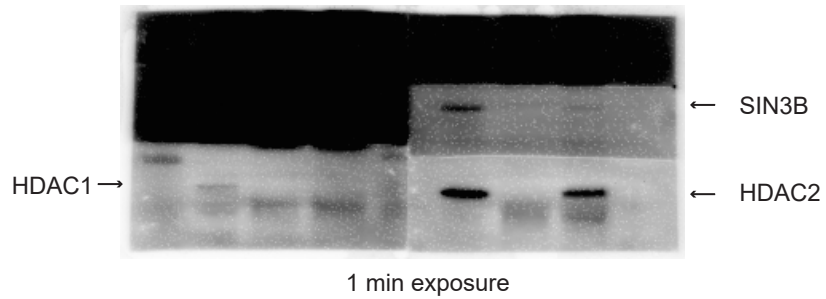
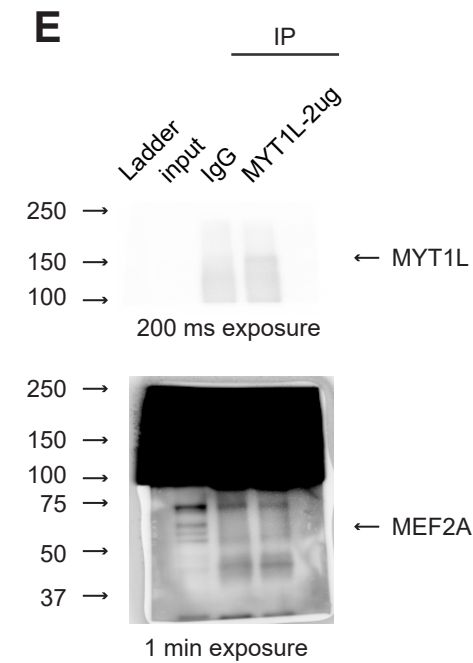
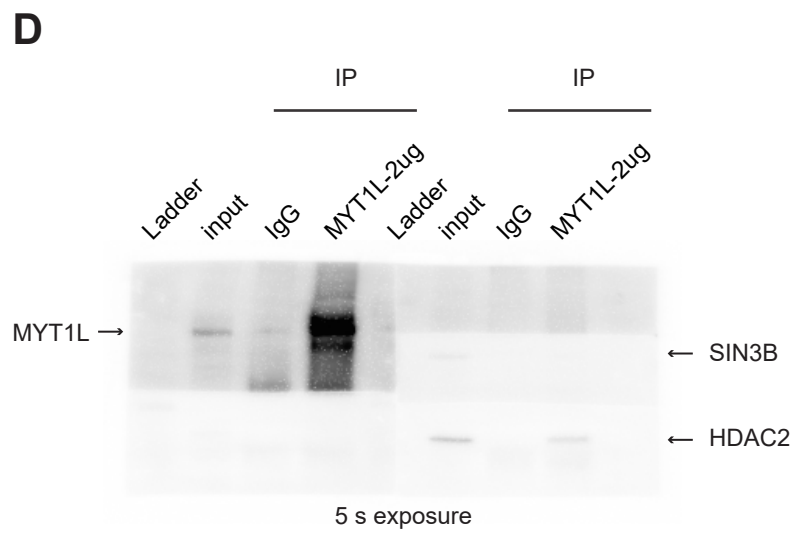
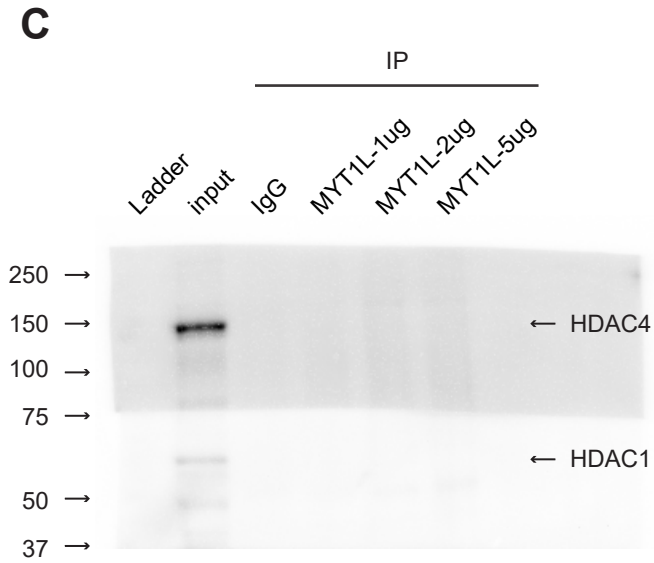
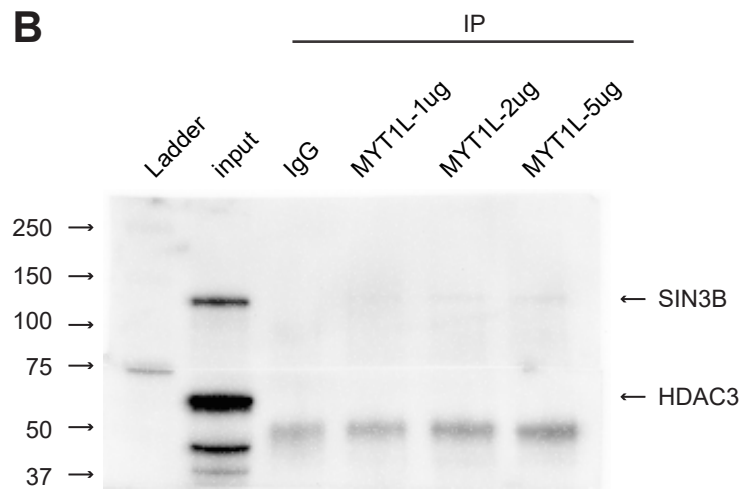
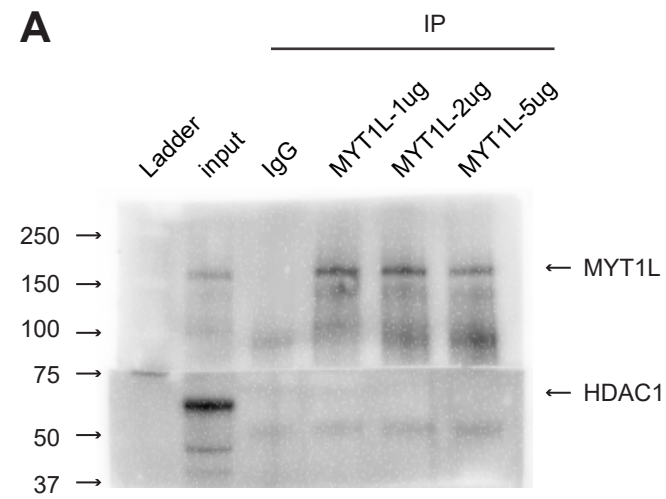
Supplemental Figure 5: MYT1L loss increases activation marks of its bound enhancers. (A) MYT1L Het PFC has reduced MYT1L binding at active (top) and poised (bottom) enhancers. (B) MYT1L loss increases its bound active (left) but not poised (right) enhancers' chromatin accessibility. (C) MYT1L bound active enhancer DARs have a higher percentage of DARs that increase accessibility than MYT1L unbound active enhancer DARs. (D) MYT1L bound poised enhancer DARs have a higher percentage of DARs that increase accessibility than MYT1L unbound poised enhancer DARs. (E) MYT1L Het PFC has higher levels of H3K4me1 at both active (left) and poised (right) enhancer targets compared to WTs. (F) MYT1L Het PFC has higher levels of H3K27ac at both active (left) and poised (right) enhancer targets compared to WTs. * $p < 0.05$, ** $p < 0.01$, *** $p < 0.001$, **** $p < 0.0001$.



Supplemental Figure 6: MYT1L loss alters H3K4me3 landscape across the genome. (A) Volcano plot showing differential enrichment analysis identified 1110 diff-H3K4me3 peaks in Het PFC. (B) Distribution of down and up-regulated diff-H3K4me3 peaks within the MYT1L- and MYT1L+ categories. (C) GO analysis on down-regulated diff-H3K4me3 peaks bound by MYT1L and (D) up-regulated diff-H3K4me3 peaks bound by MYT1L. (E) Mean ATAC-seq signals of MYT1L+ diff-H3K4me3 promoter peaks (left: up-regulated peaks, right: down-regulated peaks) (F) Mean ATAC-seq signals of MYT1L+ diff-H3K4me3 non-promoter peaks (left: up-regulated peaks, right: down-regulated peaks). (G) Functions of MYT1L targets showing up-regulation in both RNA-seq and H3K4me3. * $p < 0.05$, ** $p < 0.01$, *** $p < 0.001$, **** $p < 0.0001$.



Supplemental Figure 7: MYT1L loss alters H3K4me1 landscape across the genome. (A) Volcano plot showing differential enrichment analysis identified 1110 diff-H3K4me1 peaks in Het PFC. (B) Distribution of down and up-regulated diff-H3K4me1 peaks within the MYT1L- and MYT1L+ categories. (C) GO analysis on down-regulated diff-H3K4me1 peaks bound by MYT1L and (D) up-regulated diff-H3K4me1 peaks bound by MYT1L. (E) Mean ATAC-seq signals of MYT1L+ diff-H3K4me1 promoter peaks (left: up-regulated peaks, right: down-regulated peaks) (F) Mean ATAC-seq signals of MYT1L+ diff-H3K4me1 non-promoter peaks (left: up-regulated peaks, right: down-regulated peaks). (G) Functions of MYT1L targets showing up-regulation in both RNA-seq and H3K4me1. * $p < 0.05$, ** $p < 0.01$, *** $p < 0.001$, **** $p < 0.0001$.



Supplemental Figure 8: Full western blot images of Co-IP experiments. (A) Co-IP shows MYT1L does not interact with HDAC1. (B) Co-IP shows MYT1L interacts with SIN3B but not HDAC4. (C) Co-IP shows MYT1L does not interact with HDAC1 and HDAC4. (D) Co-IP shows MYT1L interacts with SIN3B and HDAC2 but not HDAC1. (E) Co-IP shows MYT1L does not interact with MEF2A.